Electro-Drawn Drug-Loaded Biodegradable Polymer Microneedles as a Viable Route to Hypodermic Injection

Raffaele Vecchione, Sara Coppola, Eliana Esposito, Costantino Casale, Veronica Vespini, Simonetta Grilli, Pietro Ferraro, and Paolo Antonio Netti**

Hypodermic needle injection is still the most common method of drug delivery despite its numerous limitations and drawbacks, such as pain, one-shot administration, and risk of infection. Seeking a viable, safe, and pain-free alternative to the over 16 billion injections per year has therefore become a top priority for our modern technological society. Here, a system that uses a pyroelectric cartridge in lieu of the syringe piston as a potential solution is discussed. Upon stimulation, the cartridge electro-draws, at room temperature, an array of drug-encapsulated, biodegradable polymer microneedles, able to deliver into hypodermic tissue both hydrophobic and hydrophilic bioactive agents, according to a predefined chrono-programme. This mould-free and contact-free method permits the fabrication of biodegradable polymer microneedles into a ready-to-use configuration. In fact, they are formed on a flexible substrate/holder by drawing them directly from drop reservoirs, using a controlled electro-hydrodynamic force. Tests of insertion are performed and discussed in order to demonstrate the possibility to prepare microneedles with suitable geometric and mechanical properties using this method.

1. Introduction

Microneedles are well known in the pharmaceutical field as effective and pain-free micro-scale devices employed for transdermal vaccination and drug delivery.[1] In particular, vaccine delivery via microneedles has attracted considerable attention, since it elicits immune responses comparable to (or better than) traditional skin delivery via hypodermic injection.[2] Microneedles have been studied in vitro, in animals and in humans for a variety of applications and there are also examples of metal microneedles in phase 3 clinical trials.[3] In general, metal microneedles have been engineered and used for the transdermal delivery of several biomolecules (e.g., proteins, vaccines, DNA, antibodies, or genes),[4–8] and used either as drug-coated or hollow microneedles.[6–10] However, a major limitation of metal microneedles is the risk associated with breakage;[3] there are also issues associated with drug administration. In the case of drug coated surfaces, the major problem is represented by low-payload capability, whereas, in the case of hollow microneedles, the problem resides in the complexity of the infusion system. Dissolving or degradable microneedles have been therefore developed and proved able to release encapsulated pharmaceutical molecules into the skin after dermal insertion.[11–14] These microdevices have been also proposed for influenza vaccination as a method to improve immunogenicity with respect to conventional intramuscular injections.[15] Unfortunately, the production technologies for polymer microneedles present some difficulties that often prevent their market spreading. First, most polymer microneedles are fabricated by stamp-based methods characterized by costly and time consuming multiple steps, such as: fabrication of a complex master structure; fabrication of a three-dimensional (3D) mould; filling of a polymer with the drug to be encapsulated; setting of the polymer and separation of the polymer microneedle patch from the 3D mould.[13,16–18] Moreover, since microneedles must have sufficient strength to penetrate the skin,[13,19] only high molecular weight polymers can be used; their setting parameters, however, might pose severe technical limitations. Indeed, high processing temperatures limit the use of thermolabile drugs.[13,20] On the other hand, solvent casting at room temperature is a complex and time-consuming procedure.[14,21] Casting at room temperature of photocurable polymers has also been proposed,[16,17] but UV can impair the activity of the incorporated drug, and photoinitiators are potentially toxic.[21]

Recently, a novel drawing lithography technique has been proposed as a potential solution to some of the above issues.[22,23] However, such process free from replica moulding creates 3D microstructures from two-dimensional (2D) thermosetting polymers, thus still suffering from the limitations of high processing temperature. In addition, microneedle formation strongly relies on the dynamic interaction between frame

Dr. R. Vecchione, S. Coppola, Dr. V. Vespini, Dr. S. Grilli, Dr. P. Ferraro
Istituto Nazionale di Ottica,Unità di Napoli
Via Campi Flegrei 34, 80078, Pozzuoli Napoli, Italy
E-mail: simonetta.grilli@ino.it

Dr. R. Vecchione, E. Esposito, Prof. P. A. Netti
Center for Advanced Biomaterials
for Health Care – IIT@CRIB
Istituto Italiano di Tecnologia – Largo Barsanti e Matteucci
53 80125 Napoli, Italy
E-mail: paolo.netti@iit.it

S. Coppola, E. Esposito, Dr. C. Casale, Prof. P. A. Netti
Centro di Ricerca Interdipartimentale sui Biomateriali – CRIB
Università di Napoli Federico II
Piazzale Tecchio, 80 80125 Napoli, Italy

DOI: 10.1002/adfm.201303679

and fluid, which leads to a poor reproducibility compared to the mould technology. In summary, all currently used technologies to fabricate polymer microneedles show both technical drawbacks and cost issues, which limit their successful entry into the market. Here, we propose a novel non-contact and room temperature electro-drawing (ED) process for the direct and rapid fabrication of biodegradable microneedles by means of an electrohydrodynamic (EHD) process. Our technique consists of drawing the microneedles from a sessile drop of a biopolymer solution by using EHD forces. This approach overcomes all the limitations deriving from the micro-casting and the drawing lithography approach, since no hazardous temperatures, no multi-step filling process and no UV are required. In fact, biopolymers are processed from a solution at temperatures in the range of 20–40 °C and are shaped directly into microneedles in a single step. The contact-free method proposed here avoids the use of moulds and could be suitable for the microengineerization of polymer microneedles. It is shown that, working on the formulation of polymer solution or water in oil emulsion, it is possible to encapsulate both hydrophobic or/and hydrophilic compounds at dosages of therapeutic interest. The results demonstrate the formation of microneedles of variable shapes onto flexible polymer strips that can be easily inserted in a cuff as a sort of disposable cartridge for transdermal drug delivery. Furthermore, various insertion tests have been performed with the aim to show the effectiveness of the indentation process. The porous structure resulting from processing water in oil emulsion can be tuned to modulate polymer degradation and thus control the profile release.

2. Results and Discussion

Electro-drawing was innovatively used to prepare dissolving biodegradable microneedles made of poly(lactic-co-glycolic acid) (PLGA). Detailed descriptions of the fabrication process, characterization and analysis of microneedles are reported in Section 2.1. Moreover, as discussed in the following Section, we show that the electro-drawn microneedles have geometric and mechanical properties suitable to effectively indent and penetrate the stratum corneum of cadaver skin taken from pigs, reaching the dermis. Experimental results reported here make evident that electro-drawn microneedles are appropriate biodegradable devices for drug delivery.

2.1. Electro-Drawing Of Degradable Microneedles

The set-up used for the ED process is relatively easy to assemble and consists basically of a polar dielectric crystal (lithium tantalate, LT) facing the starting polymer reservoir drop at a controlled distance. The operation principle of the fabrication process relies essentially on the use of the pyroelectric effect generated onto the LT crystal that, consequently, operates as the driving plate (DP).[24–26] The starting polymer drops could be deposited onto a microscope glass slide or, in case of flexible arrays of microneedles, onto a poly(dimethyl-siloxane) (PDMS) strip, as described in **Figure 1**a. An appropriate thermal stimulus applied to the DP generates an electric field that induces an EHD force responsible for destabilizing and drawing the polymer into a microneedle shape. In fact, it is well known that liquid drops subject to EHD forces generated by external electric fields deform into the so-called Taylor cone,[27,28] assimilated, in this case, to the form of a microneedle by appropriately manipulating the electro-drawing force. The deposition of multiple base drops allows the formation of microneedles under array-like configurations. In fact, the reservoir drops dispensed, using a syringe pump, directly onto the substrate of interest are subjected in lock step to the electro-drawing process under the action of the pyro-EHD force. The local heating induced onto the drop reservoir by the thermal stimulus applied to the crystal was measured during the experiment by colour change using a thermo camera (Flir i7) and it is <40 °C. The DP is mounted onto a precision translation stage to appropriately control the distance from the drop reservoir and, consequently, the drawing force. A conventional side illumination was used to monitor the process in real time (see Experimental Section). The microneedle fabrication is accomplished in three main steps, as shown in Figure 1a: deposition of the drop reservoirs; activation of the EHD force; evaporation of the solvent. The final result was an array of microneedles formed onto a flexible strip. During the drawing process, the liquid cone becomes solid due to the fast evaporation of the solvent, thus giving the microneedles the desired shape. A post thermal treatment (40 °C for 10 min) can be applied to the microneedles before complete solvent removal to get them a sharper tip and inducing at the same time a shrinkage that leads to an improvement of the aspect ratio. The geometry of the cone is governed by the ratio of the surface tension to the electrostatic attraction. The fabrication process can be controlled through the appropriate handling of the EHD process. The process described above shows for the first time, to the best of our knowledge, the usage of EHD force for drawing a drop of polymer solution directly into a microneedle shape. Overall, in principle the method can be applied to any type of polymer with different biodegradation time even in the case of highly viscous polymer.

In the applications described in our work, the reservoir consisted basically of a biocompatible mixture of three main components: a biodegradable copolymer PLGA, widely used for therapeutic devices, dimethyl carbonate (DMC) as a solvent and different kinds of molecules, such as Rhodamine 6G, Nile Red and rhodamine labelled human serum albumin (HSA) acting as model active compounds.

We focused on PLGA, a widely used material for microneedles, because of its properties in terms of mechanical strength and biodegradation.[29] A preliminary investigation was performed on the formation of single microneedles from PLGA solutions in order to characterize the main conditions that regulate the microneedle formation, basically the ED process. Typically, the base drop was deposited onto a PDMS strip and had a volume ≤0.1 µL. The distance between the reservoir and the DP was crucial and depended on both the volume and the contact angle of the base drop. The DP was heated locally in correspondence of the base drop, while approaching the base reservoir. Since the EHD force depends on the viscosity of the fluid, the control of this parameter was crucial for the successful formation of microneedles with the necessary shape and strength to penetrate the skin. Therefore, the ED experiments

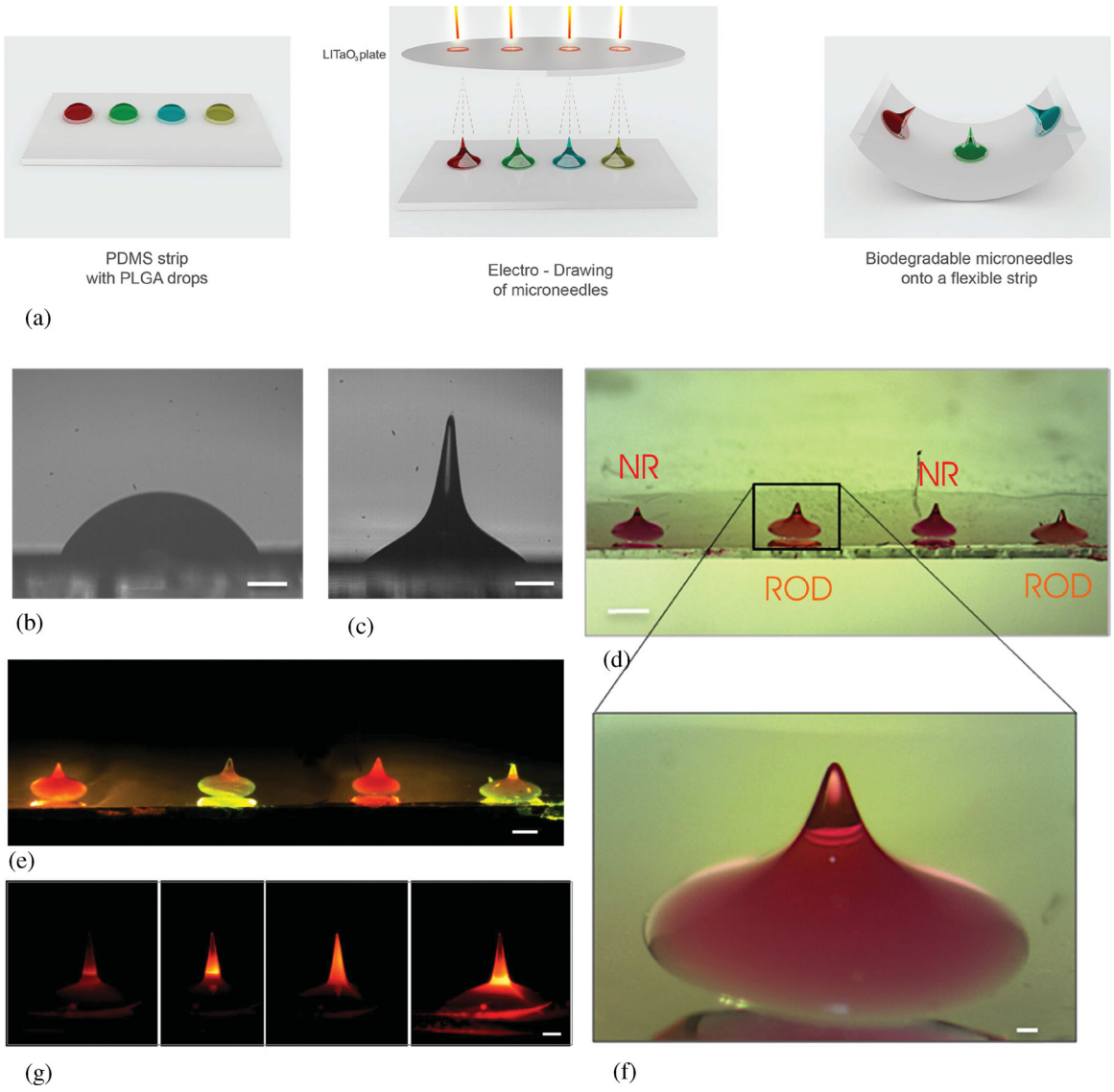

Figure 1. a) Schematic view of the biodegradable microneedle fabrication process onto flexible substrate; b) bright light image of a typical sessile drop of the PLGA biopolymer deposited onto a flat substrate before starting with the electro-drawing process (scale bar 200 μm); c) bright light image of a typical microneedle, corresponding to the reservoir drop of figure b and electro-drawn under the action of the pyro-EHD pressure (scale bar 200 μm); d) white-lamp (scale bar 1 mm); and e) fluorescence stereo-microscope images of an array of multi-drug microneedles onto a microscope glass flat substrate (Nile Red (red) and Rhodamine 6G (yellow)) (scale bar 300 μm); f) magnified view of a Nile Red microneedle (scale bar 70 μm); g) fluorescence scan of a typical microneedle along different vertical planes, the laser beam is moved from the base to the tip of the cone in order to show the photoluminescence emission of the microstructure: all this information is summarized in the last frame where a fluorescence image of the needle in total is obtained using a different angle for the incident laser beam (scale bar 100 μm).

were performed with PLGA samples dissolved in solvent with different mixing ratios in order to characterize the drawing behaviour. A proper range of polymer concentrations was chosen, from 20 to 30% w/v, to guarantee suitable viscosities in the range of around 80 to 240 $mm^2\ s^{-1}$ (measured by using an Ubbelohde viscosimeter). Higher concentrations increased the solution viscosity dramatically, making the electric field unable to deform the drop. Conversely, at lower concentrations, viscosity was too low and as a result the polymer cone was not stable. Therefore, all tests reported hereafter are obtained with 25% w/v of polymer solution. Figure 1c shows the side view of a typical microneedle immediately after formation, while Figure 1b shows the corresponding drop reservoir. The PLGA reservoir appears to clearly deform into a shape consisting of a base preserving the diameter of the starting drop and a sharp conical tip very similar to a microneedle. The chromophores embedded into the polymer made the visualization of the microneedles easier under UV illumination.

Figure 1d,e shows two stereo-microscope images (bright light and fluorescence excited by a laser source of 325 nm) of a typical row of electro-drawn microneedles containing Nile Red (two red microneedles NR) and Rhodamine 6G (two yellow microneedles ROD). The distribution of Nile Red inside the microneedles appears notably more uniform than Rhodamine

6G, due to its molecular polarity and therefore to its solubility in PLGA, even with a double concentration, as expected. Figure 1f shows a magnified view of the electro-drawn microneedles. A microneedle obtained with the method of the post thermal treatment to fasten the evaporation is reported in Figure 1g, which shows a sequence of side views of a single Nile Red microneedle acquired during the vertical scan of the microneedle by the laser beam used as an illumination source. These results demonstrate the capability of the ED to embed hydrophobic compounds into the polymer microneedle during the drawing process. On the same microneedle an in fluorescence analysis was also performed (see Supporting Information, Figure S1a–e) in order to assess the uniform distribution of the chromophore.

It is important to note that this method provides high degrees of freedom in moulding the shape of the microneedles. The polymer microneedle was formed in a single step by controlling the distance between the base and the DP. In particular, starting from the volume V of the drop reservoir we defined a critical distance D_c, so that the process takes place for values of distance shorter than the critical one [30] as expressed in:

$$D_c = \left(1 + \frac{\vartheta}{4}\right) V^{1/3} \quad (1)$$

Under these conditions, controlling the volume of the drop reservoir with a contact angle θ and the critical distance, it is possible to control the height of the microneedle produced. The microneedle height, h, is measured considering only the cone without the pedestal. For base drops of 0.05 µL < V < 0.1 µL, the typical microneedle height was 300 µm < h < 500 µm, which falls within the range used for indentation applications.[9,10,12–14] The method also allows controlling microneedle height and aspect ratio as a function of drops. As shown in **Figure 2**a,b, the microneedle height increases with the volume of the drop and the aspect ratio h/b can be modulated accordingly. The increase of the aspect ratio with the drop volume is most probably due to the fast consolidation of the walls with respect to the inner core that feeds the height increase under the persistent electric field. In Figure 2c the post-treatment microneedle profile (black) is overlapped with the original one (light gray). This treatment also reduces the pedestal volume under the cone.

An alternative configuration was implemented—in a mass-production perspective—in order to obtain a more controlled fabrication of microneedle arrays by the EDS. An array of PDMS pillars (see Experimental section) was used as a multiple base to improve the uniformity of the base drops and, consequently, that of the microneedles (see the scheme in the Supporting Information, Figure S2). Figure 2d,e show the side view of a microneedle while being drawn from the pillar-based reservoir (Figure 2d) and a fluorescence image of one electro-drawn microneedle (Figure 2e) with no post thermal treatment. In this case, the volume of the drop reservoir has been increased in the range of 0.3 µL < V < 1.8 µL; as a direct consequence, the microneedle height grows in the range of 400 µm < h < 800 µm. Thanks to the use of PDMS pillars, the density of microneedles per area can be dictated by the distance between pillars and can therefore be easily controlled. Alternatively, it would be possible to control the spacing period using the ED method, thus controlling the self-assembly of a highly viscous polymer[25] and leading to the fabrication of a tightly spaced microneedle array.

Since most of the therapeutics of interest are hydrophilic, we have adapted our technique to encapsulate any kind of hydrophilic compound in the microneedle. To this end, the PLGA solution was mixed with a water solution containing HSA labeled with Rhodamine 6G used as probe, to create a water-in-oil emulsion. The emulsion was then successfully electro-drawn (see Supporting Information, Figure S3a) to generate a needle with embossed protein loaded microcavities (Figure S3b, Supporting Information). The height was increased thanks to the post thermal treatment combined with the larger volume confined onto PDMS pillar. The dimension and the extension of these hydrophilic compartments appearing as insulated micrometric pores (Figure S3b, Supporting Information) can be tuned by the composition and distribution of water droplets within the original emulsion. Micrometric porosity within the needle structure also affects PLGA degradation rate and thus the drug release kinetics. In this view, it may be possible to tune the drug release profile by tailoring the porous microstructure adapting the emulsification conditions.[31]

The microneedles described so far present a not optimal distribution of bioactive agents. Indeed, drug is uniformly distributed throughout the whole microneedle with obvious unusable portion of drug loaded in the pedestal region. To improve the drug distribution within the needle regions, we succeeded in loading only the cone of the microneedle by using a two-stage dispensing procedure. A small drug-containing water-in-oil emulsion drop, corresponding to the volume of the needle's cone, was dispensed on the top of a drop of drug-free PLGA solution. The resulting composite drop was successfully electro-drawn to obtain a needle with a drug-encapsulated porous cone and a compact drug free pedestal. Microneedle structure and dye distribution are clearly shown by the optical stereo microscope analysis, **Figure 3**a. The separation of the two regions, cone and pedestal, is even more evident by the confocal optical analysis reported in Figure 3b. Also in this case the microneedle was obtained onto a PDMS pillar combining a post thermal treatment. In particular, the details on the distribution of the hydrophilic bioactive compound are reported in Figure 3c, which is a magnification of the previous image.

A slight evolution of the two-stage dispensing procedure could also allow for the implantation of the microneedle cones in the tissue with possible immediate patch removal by introducing a separating and fast degradable layer between the two drops; the microneedle could then be inserted into the skin layer with rapid degradation of the interface layer.[32] Doing so, the pedestal may be separated from the drug-loaded microneedle cone leaving it inserted in the skin when a long dissolving time is required.

2.2. Skin Indentation by PLGA Electro-Drawn Microneedles

To serve as a substitute for a hypodermic needle, a microneedle should penetrate the 10–20 µm thick stratum corneum, without

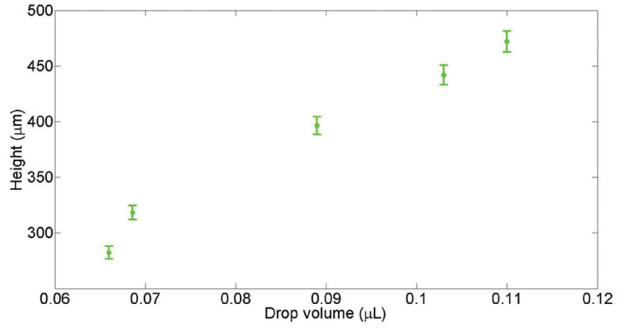

(a)

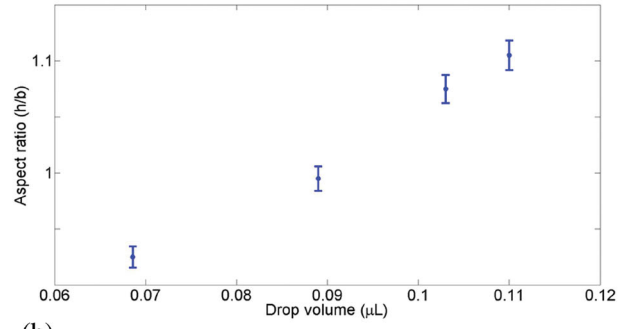

(b)

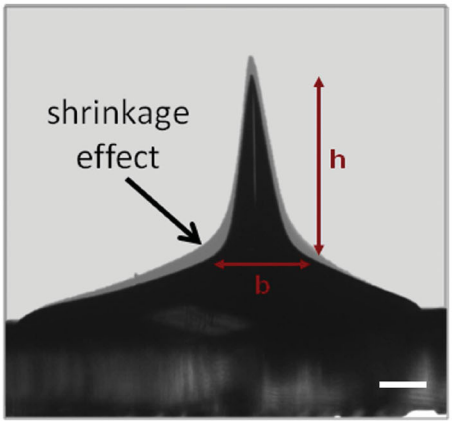

(c)

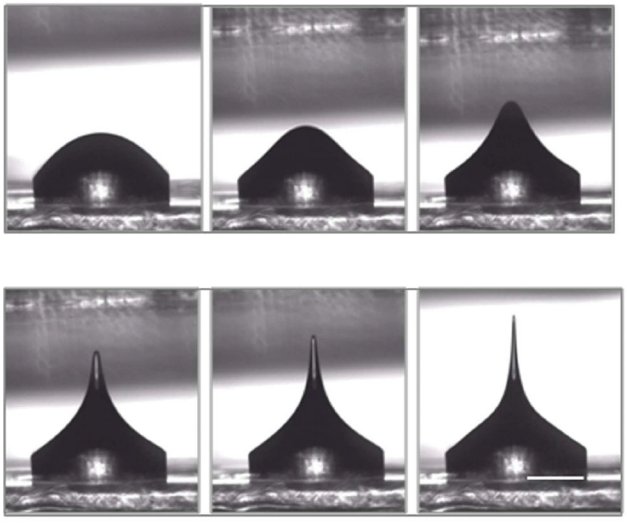

(d)

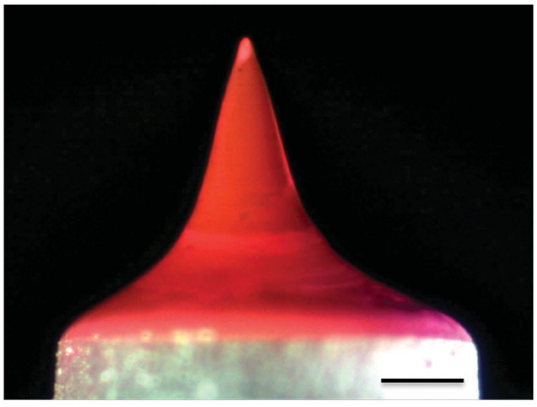

(e)

Figure 2. a) Plot of microneedle height; and b) aspect ratio as a function of volume of the corresponding reservoir drops directly deposited onto a flat microscope substrate and obtained by thermal post fabrication treatment; c) post-treatment profile (black) overlapped with the initial one (light gray) showing the possibility to improve the aspect-ratio for the fabrication of a sharper tip (scale bar 100 μm); d) evolution in time of the fabrication process using micropillars as the base of the microneedle (scale bar 200 μm): the use of micropillars leads to improve the needle formation containing the drop reservoir and limiting the pedestal during the electro-drawing process; e) magnified and fluorescence image of one electro-drawn microneedle onto a polymer micropillar (scale bar 100 μm).

breakage. Preliminary indentation experiments were performed into model materials, such as wax (see Supporting Information Movie 1) and agarose gel (see Supporting Information Movie 2) in order to test the hardness of the microneedles. The agarose gel offers an ideal test bed because it can be produced by controllable mechanical properties, while its transparency allows to view microneedle penetration in real time.[33] **Figure 4**a,b show the microneedles while penetrating the agarose and just after ejection, respectively (see Supporting Information Movie 3). The results show that microneedles about 300 μm high can penetrate agarose at a depth directly corresponding to the cone height. No breakage or bending was observed either in this case or for other

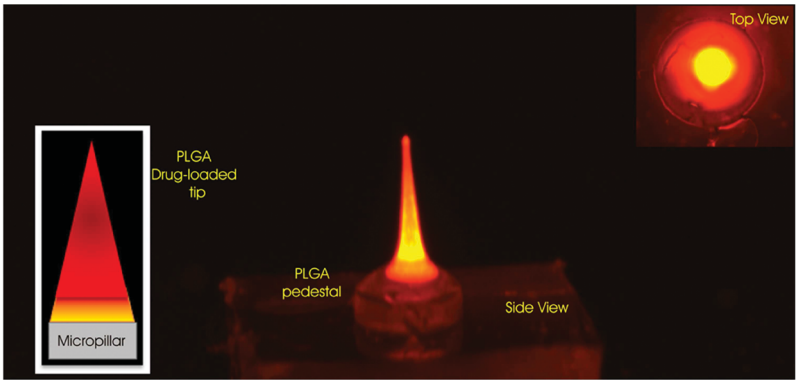

(a)

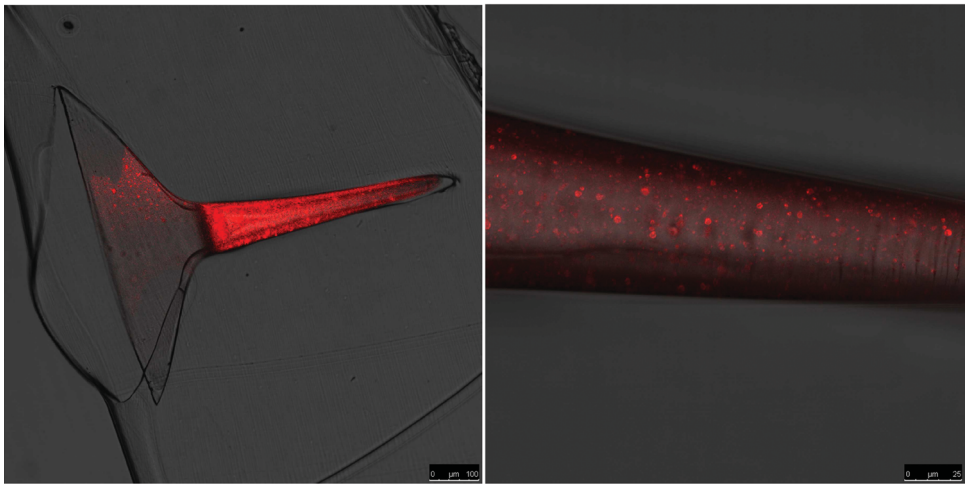

(b) (c)

Figure 3. a) Fluorescence optical microscopy image of a microneedle produced by overlapping an emulsion drop loaded with rhodamine labeled HAS onto a first drop of pure PLGA solution. The fluorescene image of the side view is compared with a schematic to better explain the needle composition. The pure PLGA solution is used for the fabrication of the pedestal, while the cone is formed from the emulsion drop deposited in a second step over the pure PLGA reservoir; b) optical confocal image of a slice of the microneedle (scale bar 100 μm); and c) magnification of a portion of the cone (scale bar 25 μm).

lengths and aspect ratios of the microneedles during the insertion tests. Then, indentation experiments were performed into real skin by inserting the Nile Red loaded microneedles obtained with post-thermal treatment into pig cadaver skin and by removing them after 15 min. The indentation was performed by tightening the flexible strip containing microneedles (see Figure 4c) onto the skin previously stretched onto a cylindrical support to emulate real conditions of use. Specifically, the necessary force to produce the indentation was of around 0.01 N per microneedle, much lower than forces (>1 order of magnitude) typically known to produce PLGA microneedle breakage.[34] The effectiveness of the indentation is confirmed by the cross sectional image of the stained skin at the site of microneedle penetration (see Experimental Section). The dermis was clearly reached by the microneedles, thus confirming its potential use for drug delivery, Figure 4d,e.[35] The insertion depth was in agreement with the dimensions of the microneedles used for test, which showed lengths of around 400, 500, 450 μm, respectively (see Supporting Information, Figure S4). In particular, they were able to penetrate all the layers of the epithelium and part of the papillary dermis. It is important to note here that the technological simplicity of the technique would provide a significant breakthrough in the clinical development of biodegradable microneedles. In principle, the entire procedure could be carried out by a single person with a portable kit, equipped with a pyroelectric crystal, micrometric controlled translation stages and integrated micro-heaters, in order to produce personalized microneedle patches for pharmaceutical self-administration.

3. Conclusion

In conclusion, this paper presents an electro-drawing (ED) approach for the fabrication of sharp, dissolving microneedles directly from a liquid polymer reservoir, moulding-free and contact-free. Model drugs can be embedded at room temperature in drop reservoirs, drawn to form microneedles at no more than 40 °C and successfully delivered via indentation into the skin. The technique allows for the encapsulation of

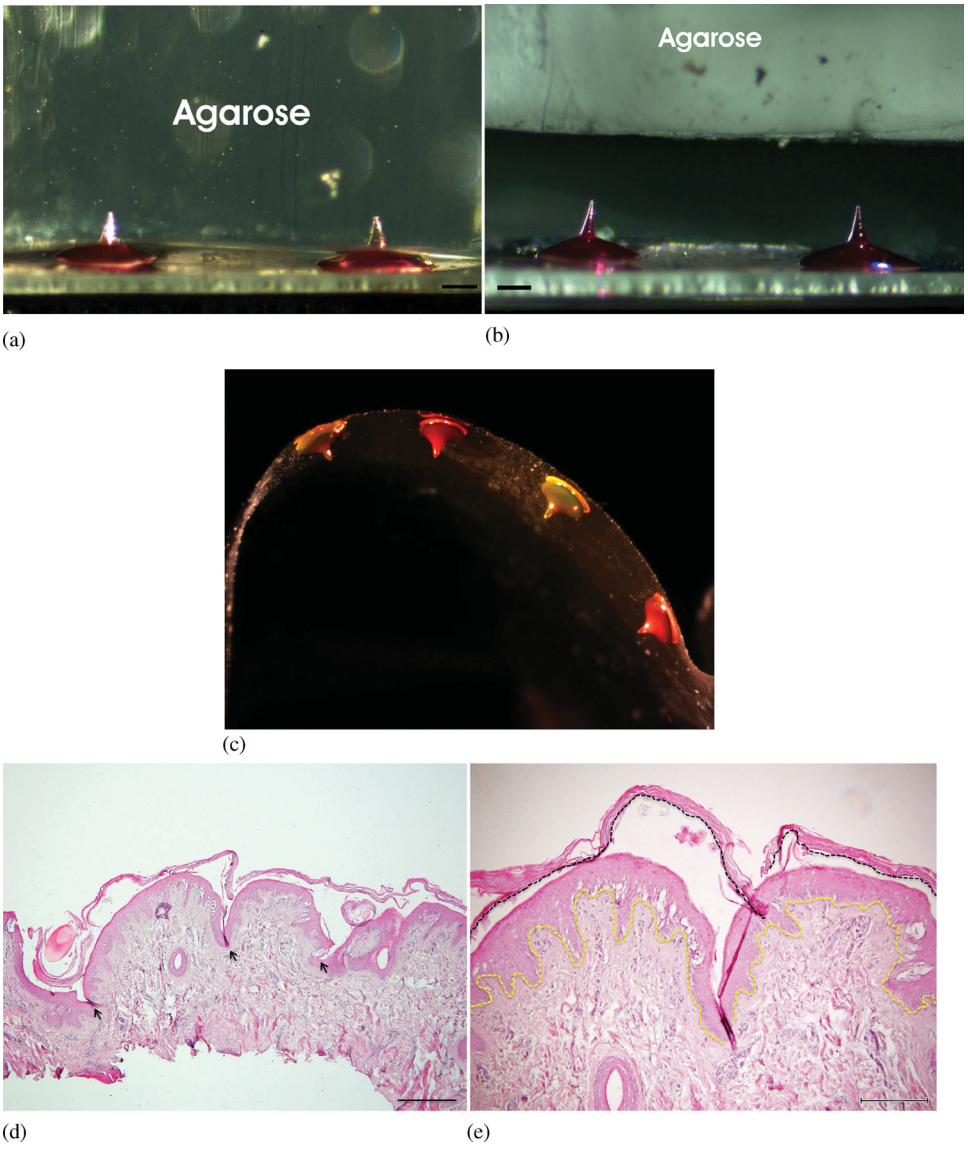

Figure 4. a) Real time indentation test of microneedles in the agarose gel used as model material (scale bar 200 μm); and b) visualization of the integrity of the microneedles just after penetration (scale bar 200 μm): the microneedle on the left side appears as slightly bending with respect to the central axis before and after insertion; c) flexible multi-drug therapeutic cuff; d) cross-sectional image of the skin after microneedle removal and skin fixing in formaline at 10 wt% with black arrows indicating the indented areas (scale bar 500 μm); e) magnification of central indentation and complete image where dashed black line indicates the stratum corneum and dashed yellow line indicates the basal membrane (scale bar 200 μm).

both hydrophobic and hydrophilic compounds. Hydrophobic drugs are entrapped in the polymeric phase, whereas hydrophilic compounds are encapsulated in microcavities created within the polymeric phase. Microneedle patches are formed directly onto a flexible, disposable strip that is inserted into a cuff, overcoming the technological limitations of both micro-casting and drawing lithography and opening new frontiers in the field of transdermal delivery. In addition, microneedle fabrication is made easy, mould-less, nozzle-less, making way for homemade patches and customized therapies. On-demand and cost-effective microneedles could be obtainable in-situ directly at the point of care, thus replacing the traditional syringes.

4. Experimental Section

Fabrication of Microneedles: Poly(lactic-co-glycolic acid) 50 : 50 (PLGA RESOMER RG 504H, 38 000–54 000 Dalton, Boeringer Ingelheim) was dissolved in dimethyl carbonate (20–30 w/v, DMC 99% Sigma-Aldrich). Then, drops of polymer solution were deposited on poly(dimethyl-siloxane) (Dow Corning 184 Sylgard) used as a flat flexible substrate or onto PDMS pillars integrated on the same flexible substrate. A syringe pump (Harvard apparatus – Plus 11) was used for the dispensing with imposed rate 0.1 $\mu L/min^{-1}$, connected to a capillary of inner diameter 500 μm, and then positioned on a platform of translation stage under a lithium tantalite crystal (Optical grade LiTaO3 wafer, z-cut, 0.5 mm thickness, both side polished, Roditi International Corporation Ltd) that was locally heated until 80 °C in correspondence to the drops in order to draw them and create the cone-like shape. A 5× microscope objective

and a high-speed digital CMOS camera (pixel size 12 mm × 12 mm, frame rate of 500 frames s^{-1} with 1280 (H) × 1024 (V) spatial resolution) were used to capture side-view pictures and videos during microneedle formation. After the electro-drawing process, microneedles can be kept at temperature of about 40 °C for 10 min, to accelerate solvent evaporation and fix microneedle shape. In some preparations polymer solution was loaded with Nile Red (2 μg per mg of PLGA) technical grade, Sigma-Aldrich) and Rhodamine 6G (1 μg per mg of PLGA, Dye content ≈95% Sigma-Aldrich).

To obtain microneedles with a porous microstructure to embed hydrophilic compounds, a water solution was prepared with lecithin (Lipoid E80, Lipoid AG), a biocompatible surfactant, and human serum albumine (HSA, lyophilized powder, fatty acid free, globuline free, ≥95%, Sigma-Aldrich) labelled with rhodamine (5(6)-Carboxy-X-rhodamine N-succinimidyl ester, Sigma-Aldrich) dissolved in water (lecithin 20 mg mL^{-1}, HSA 40 mg mL^{-1}). This aqueous phase was emulsified in the PLGA solution (40 wt%) by using an immersion sonicator (Ultrasonic Processor VCX500 Sonic and Materials) for 20 s at 30 wt% of power. Following steps such as deposition and drawing of drops solution, are unchanged. To localize the active compound in the microneedle cone, a method characterized by a double dispensing process was implemented, where a first drop is deposited on the pillar and then followed by the deposition of a second drop of a volume 1/10 (v/v) with respect to the first one and containing the active compound.

Fabrication of Master for Flexible Support: The negative of the array of pillars was tooled on PMMA substrate by using the micromilling technique (Mini-Mill/GX, Minitech Machinery Corporation), to form a cylindrical cavity with a diameter of 700 μm and a depth of 200 μm (different sizes are possible). Then, a flexible layer with pillars was obtained by pouring PDMS, mixed in ratio 10:1 with curing agent on the above described master and under vacuum until complete disappearance of the air bubbles. Finally, it was cured at 80 °C for 30 min and peeled off from PMMA master.

Slicing Microneedle: To slice microneedles, they were incorporated in PDMS, cured for 24 h at room temperature, and then frozen at –120 °C in Leica CryoUltra Microtome EM-FC7-UC7. Samples were sectioned at a thickness of 10 μm for SEM analysis and 1 μm for confocal analysis.

Imaging Analysis: A morphological analysis was performed using field emission SEM (Ultra plus Zeiss) on porous microneedle slices. To avoid damage inside the samples, they were sputter coated with a 15 nm thick gold and a voltage (EHT) of 5 kV was imposed.

Then, to investigate cromophore distribution inside the microneedle, slices of samples, 1 μm thick, were analyzed with a confocal Leica TCS at 543 nm using a 25× water immersion microscope objective. Acquired images were analyzed using ImageJ (Java-based image processing program developed at the National Institutes of Health).

Indentation Tests: A small block of wax (paraffin wax, Sigma-Aldrich) and of agarose gel (4% agarose gel, Sigma-Aldrich) prepared on the day of use were fixed over a microscope slide and connected to a computer-controlled *x*, *y* axes translation stage, with movement velocity of 0.7 mm s^{-1} facing down the polymer strip with the microneedle (wax, Supporting Information Movie 1; agarose gel, Supporting Information Movie 2). The indentation experiment was visualized in situ by an optical set-up. In particular, by controlling the distance in real time the blocks were put in contact with the microneedle tip until it reached the microneedle base. In the case of agarose gel a conventional blue collimated led light (wavelength of 470 nm and beam power around 400 mW) illuminated the cross-section of the microneedle, while a digital CMOS video camera (pixel size 12 μm × 12 μm; frame rate of 500 frames s^{-1} with 1280 (H) × 1024 (V) spatial resolution) was used for recording the process. A 5× microscope objective was adopted to image the process on the CMOS sensor (Supporting Information Movie 3).

Then, a series of three microneedles was inserted in a full thickness cadaver pig skin without subcutaneous fat that was shaved with cream and washed in a solution of phosphate buffered saline (PBS, Lonza); finally, it was placed on absorbing paper for a few minutes to eliminate the water in excess. The indentation test was carried out with a system emulating the application of the microneedle patch through a bracelet. Pig skin was positioned onto a cylindrical tube, with a diameter of about 5 cm, and gently stretched by hand. Microneedles previously attached on the plastic plate of the bracelet were pressed onto the skin and kept close by means of elastic bands and Velcro for 10 min. The pressure exerted by tightening the cuff was measured by introducing a pressure sensor (CZN-CP1, TME electronic components) between the cuff and the flexible layer supporting the microneedles.

Histological Analysis: After indentation, the microneedles were removed and the skin was fixed in a solution of neutral buffered formaline (10 wt%, Bio-Optica) for 24 h, dehydrated in an incremental series of alcohol (75, 85, 95 and 100, and 100 wt% again, each step 20 min at room temperature), treated with xylene (histological grade, Sigma-Aldrich) and then embedded in paraffin (Bio-Optica). Successively, samples were sectioned at a thickness of 6 μm, and stained with hematoxylin (Bio-Optica) and eosin (Bio-Optica), and finally the sections were mounted with Histomount Mounting Solution (Invitrogen) on coverslips and the morphological features of the constructs were observed with a light microscope (BX53; Olympus).

Supporting Information

Supporting Information is available from the Wiley Online Library or from the author.

Acknowledgements

R.V. and S.C. contributed equally to this work. The authors thank Andrea Finizio for the fluorescence images and the realization of the supplementary movies with technical and artistic expertises. The authors thank Fabio Formiggini for technical assistance in the acquisition of confocal images and Valentina Mollo for her patience in the realization of microneedles' slices. Moreover, the authors thank Valentina La Tilla for the graphical abstract realization and Roberta Infranca for her precious and careful proofreading. Finally, authors thank Antonelli Carmela of ASL Napoli 2 Nord, for providing pig cadaver skin taken from the butchery implant ICS (Industria Carni Sud) of Caivano, Naples (IT).

Received: October 29, 2013
Revised: January 10, 2014
Published online: February 24, 2014

[1] A. Arora, M. R. Prausnitz, S. Mitragotri, *Int. J. Pharm.* **2008**, *364*, 227.
[2] W. C. Weldon, M. P. Martin, V. Zarnitsyn, B. Wang, D. Koutsonanos, I. Skountzou, M. R. Prausnitz, R. W. Compans, *Clin. Vaccine Immunol.* **2011**, *18*, 647.
[3] S. H. Bariya, M. C. Gohel, T. A. Mehta, O. P. Sharma, *J. Pharm. Pharmacol.* **2012**, *64*, 11.
[4] G. Widera, J. Johnson, L. Kim, L. Libiran, K. Nyam, P. E. Daddona, M. Cormier, *Vaccine* **2006**, *24*, 1653.
[5] J. Hadgraft, M. E. Lane, *Phys. Chem. Chem. Phys.* **2011**, *13*, 5215.
[6] Q. Zhu, V. G. Zarnitsyn, L. Ye, Z. Wen, Y. Gao, L. Pan, I. Skountzou, H. S. Gill, M. R. Prausnitz, C. Yang, R. W. Compans, *Proc. Natl. Acad. Sci. U. S. A.* **2009**, *106*, 7968.
[7] Y. C. Kim, F. S. Quan, R. W. Compans, S. M. Kang, M. R. Prausnitz, *Pharm. Res.* **2011**, *28*, 135.
[8] J. Gupta, H. S. Gill, S. N. Andrews, M. R. Prausnitz, *J. Controlled Release* **2011**, *154*, 148.
[9] M. R. Prausnitz, *Adv. Drug Delivery Rev.* **2004**, *56*, 581.
[10] H. S. Gill, M. R. Prausnitz, *J. Controlled Release* **2007**, *117*, 227.
[11] G. Li, A. Badkar, S. Nema, C. S. Kolli, A. K. Banga, *Int. J. Pharm.* **2009**, *368*, 109.
[12] C. Baek, M. R. Han, J. Min, M. R. Prausnitz, J-H. Park, J. H. Park, *J. Controlled Release* **2011**, *154*, 138.

[13] J.-H. Park, M. G. Allen, M. R. Prausnitz, *J. Controlled Release* **2005**, *104*, 51.
[14] J. W. Lee, J.-H. Park, M. R. Prausnitz, *Biomaterials* **2008**, *29*, 2113.
[15] S. P. Sullivan, D. G. Koutsonanos, M. del Pilar Martin, J. W. Lee, V. Zarnitsyn, S-O. Choi, N. Murthy, R. W. Compans, I. Skountzou, M. R. Prausnitz, *Nat. Med.* **2010**, *16*, 915.
[16] S. P. Sullivan, N. Murthy, M. R. Prausnitz, *Adv. Mater.* **2008**, *20*, 933.
[17] L. Y. Chu, M. R. Prausnitz, *J. Controlled Release* **2011**, *149*, 242.
[18] S. D. Gittard, A. Ovsianikov, N. A. Monteiro-Riviere, J. Lusk, P. Morel, P. Minghetti, C. Lenardi, B. N. Chichkov, R. J. Narayan, *J. Diabetes Sci. Tech.* **2009**, *3*, 304.
[19] S. P. Davis, B. J. Landis, Z. H. Adams, M. G. Allen, M. R. Prausnitz, *J. Biomech.* **2004**, *37*, 1155.
[20] J.-H. Park, M. G. Allen, M. R. Prausnitz, *Pharm. Res.* **2006**, *23*, 1008.
[21] K. Tsioris, W. K. Raja, E. M. Pritchard, B. Panilaitis, D. L. Kaplan, F. G. Omenetto, *Adv. Funct. Mater.* **2012**, *22*, 330.
[22] K. Lee, J. D. Kim, C. Y. Lee, S. Her, H. Jung, *Biomaterials* **2011**, *32*, 7705.
[23] C. K. Choi, J. B. Kim, E. H. Jang, Y.-N. Youn, W. H. Ryu, *Small* **2012**, *8*, 2483.
[24] P. Ferraro, S. Coppola, S. Grilli, M. Paturzo, V. Vespini, *Nat. Nanotechnol.* **2010**, *5*, 429.
[25] S. Grilli, S. Coppola, V. Vespini, F. Merola, A. Finizio, P. Ferraro, *PNAS* **2011**, *108*, 15106.
[26] S. Coppola, V. Vespini, S. Grilli, P. Ferraro, *Lab Chip* **2011**, *11*, 3294.
[27] J. U. Park, M. Hardy, S. J. Kang, K. Barton, K. Adair, D. K. Mukhopadhyay, C. Y. Lee, M. S. Strano, A. G. Alleyne, J. G. Georgiadis, P. M. Ferreira, J. A. Rogers, *Nat. Mater.* **2007**, *6*, 781.
[28] B. de Heij, M. Daub, O. Gutmann, R. Niekrawietz, H. Sandmaier, R. Zengerle, *Anal. Bioanal. Chem.* **2004**, *378*, 119.
[29] M. Y. Kim, B. Jung, J.-H. Park, *Biomaterials* **2012**, *33*, 668.
[30] N. Maeda, J. N. Israelachvili, M. M. Kohonen, *Proc. Natl. Acad. Sci. U. S. A.* **2003**, *100*, 803.
[31] F. Ungaro, M. Biondi, I. D'Angelo, L.Indolfi, F. Quaglia, P. A. Netti, M. I. La Rotonda, *J. Controlled Release* **2006**, *113*, 128.
[32] P. C. DeMuth, W. F. Garcia-Beltran, M. L. Ai-Ling, P. T. Hammond, D. J. Irvine, *Adv. Funct. Mater.* **2013**, *23*, 161.
[33] A. Arora, I. Hakim, J. Baxter, R. Rathnasingham, R. Srinivasan, D. A. Fletcher, S. Mitragotri, *Proc. Natl. Acad. Sci. U. S. A.* **2007**, *104*, 4255.
[34] J.-H. Park, M. R. Prausnitz, *J. Korean Phys. Soc.* **2010**, *56*, 1223.
[35] L. Y. Chu, S.-O. Choi, M. R. Prausnitz, *J. Pharm. Sci.* **2010**, *99*, 4228.